Fault Analysis in Solar Photovoltaic Arrays

By

Bill N. Nunneh

21161012

A project submitted to the Department of Electrical & Electronic Engineering in partial fulfillment for the award of the Degree of
Master of Engineering in Electrical & Electronic Engineering

Department of Electrical and Electronic Engineering
BRAC University
January, 2023

Declaration

It is hereby declared that

1. The project submitted is my own original work while completing my master degree at BRAC University.
2. The project does not contain material previously published or written by another person, except where due reference is made in the text.
3. The project does not contain material which has been accepted or submitted for any other degree or diploma at a university or other institution.
4. I have acknowledged all main sources of information.

Student's Full Name & Signature:

Bill N. Nunneh
21161012

Approval

The project titled "Fault Analysis in Solar Photovoltaic Arrays" submitted by

Bill N. Nunneh (21161012)

of Spring 2021, has been accepted as satisfactory in partial fulfillment of the requirements for the degree of Master of Engineering (M.Eng.) in Electrical and Electronic Engineering, submitted on 26th January, 2023.

Examining Committee:

Supervisor:
(Member)

____
Dr. A. S. Nazmul Huda
Associate Professor
Department of Electrical and Electronic Engineering
BRAC University

Internal Examiner:
(Member)

____
Dr. Shahidul Islam Khan
Professor
Department of Electrical and Electronic Engineering
BRAC University

Departmental Head:
(Chair)

____
Dr. Md. Mosaddequr Rahman
Professor and Chairperson
Department of Electrical and Electronic Engineering
BRAC University

Abstract

Finding faults and partial shadow conditions are the key challenges for photovoltaic (PV) system. Furthermore, by being aware of how many broken modules and strings there are, the power loss can be averted. Some studies are conducted in this project to address these issues in order to distinguish between faults and partially shaded conditions as well as the quantity of mismatched modules and strings for a dynamic change in irradiation. Based on a straightforward observation of the PV array's Current versus Voltage (I-V) characteristic curve under fault conditions, the suggested approach has evolved in two key steps. Using predetermined variables that are continuously updated from PV array voltage, current, and irradiation, the type of fault is first identified. By comparing the data with theoretical predictions derived from the PV array's I-V characteristic curve, it then provides the number of short-circuited bypass diodes and open-circuited blocking diodes. MATLAB/Simulink simulations have been used to verify the suggested approach.

Keywords: Photovoltaic (PV) Array, Faults, (I-V) characteristic curve, Line-Line (LL) fault, MATLAB Simulink.

Acknowledgement

I would like to express my deepest sense of gratitude towards my supervisor, Dr. A. S. Nazmul Huda, Associate Professor, Department of EEE, BRAC University, Dhaka, Bangladesh, who has given me many suggestions, guidance, and support. I would like to thank all the staff members of the Department of Electrical and Electronics Engineering (EEE), BRAC University, for their extended cooperation and guidance.

I also want to use this opportunity to give thanks to all those who have given me support for the project and in other aspects of my study at BRAC University.

Table of Content

List of Figures

List of Abbreviations

AM	Air Mass
DC	Direct Current
GFPD	Ground Fault Prevention Device
I-V	Current vs. Voltage
I_D	Diode Current
I_S	Saturation Current
I_{SC}	Short Circuit Current
k	Boltzmann Constant
MPPT	Maximum Power Point Tracking
MPP	Maximum Power Point
PV	Photovoltaic
$R_{C,S}$	Solar cell series resistance
R_{sh}	Shunt Resistance
STC	Standard Test Conditions
T	Ambient Temperature
V_D	Diode Voltage
V_{OC}	Open Circuit Voltage

Chapter 1

Introduction

1.1 Background

Renewable energy comes from natural resources that reappear throughout time without depleting global resources. Additional benefits of these resources are their abundance, accessibility, and minimal or nonexistent environmental impact. The thermal energy found in the earth's crust, wind, solar, and solar-wind energy are a few examples. Consistent electricity from renewable sources and fuel diversity increase energy security, lower the chance of fuel leaks, and lessen the requirement for imported fuels [1]. The use of renewable energy sources is currently very popular. Research in this area has grown as a result of the need for and limited supply of conventional energy sources, as well as the creation of new energy sources. Since it seems to be one of the most promising renewable energy sources, solar energy has drawn a lot of attention as a source of power. It is unconventional for the environment and uses no gasoline [3]. A photovoltaic (PV) system's output power is affected by the weather due to its nonlinear I-V characteristic. I-V characteristics of power peaks occur at specific times [2]. The maximum power point (MPP) has been reached, and the power change rate is now zero. The MPP of a PV system changes with temperature and solar radiation; hence, it is impossible for a PV system to operate at its MPP without making the appropriate system adjustments. [1]. Solar energy is the sun's radiant heat and light, and examples of ways to harness it include solar power which may be used to generate electricity and solar thermal energy which can be used to heat water [3].

1.2 Concept of Solar Photovoltaic

The term "photovoltaic" refers to semiconductors that exhibit the photovoltaic effect and are used in the conversion of light into electricity. The creation of voltage across a semiconductor's PN junction as a result of light absorption is known as the photovoltaic effect [3]. Photovoltaic devices are the ones that are dependent on this occurrence. Semiconducting components in a solar panel absorb light energy when it is exposed to the sun. The released electrons produce the external DC current as a result of the energy that was absorbed. The coupling of the p and n layers to an external circuit causes electrons to travel from the n-layer to the p-layer [4, 5]. PV cells are composed of a minimum of two layers of a semiconducting material, frequently silicon, which has been doped with special additives. On opposing layers, there are positive and negative charges. Light that penetrates the cell generates energy that permeates every layer of the cell. According to the brightness of the light, each cell produces a particular amount of electrical power, as seen in Figure 1.1 below.

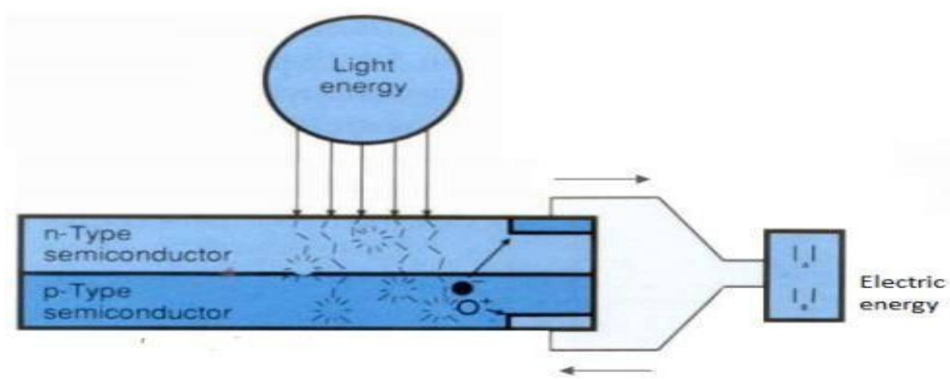

Figure 1.1 Photovoltaic Device

1.2.1 Photovoltaic Module

In a PV module, several PV cells are linked in parallel and series to enhance voltage and decrease current, respectively. The industry standard for large-scale power generation uses modules with 36 cells. A mountable device is often held together by an aluminum frame with weather-resistant edges. The electrical connection point for the module is the junction box, also known as the wire leads, which is found on the rear of the module.

1.2.2 Photovoltaic Array

A solar photovoltaic array is a setup made up of numerous solar panels that are interconnected. Individual photovoltaic cells are linked together to form photovoltaic solar panels [7]. Numerous solar panels are electrically linked together to form an array, which is a bigger photovoltaic installation [8]. Photovoltaic panels and cells convert solar energy into direct-current (DC) power. Similar to how PV cells are joined in a single panel, solar panels are connected in a single photovoltaic array. An array's panels can be connected in series, parallel, or a combination of the three; however, a series connection is frequently chosen to increase output voltage.

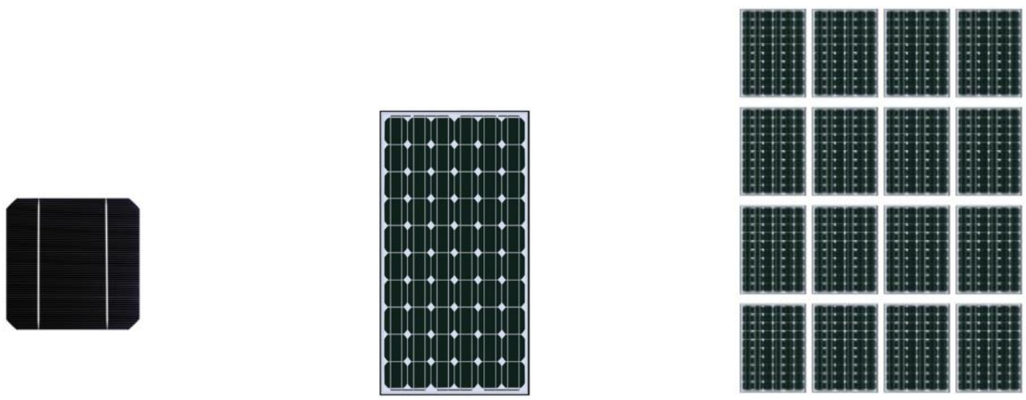

(a) Solar Cell (b) PV Module (c) PV Array

Figure 1.2 (a) Cell (b) Module (c) Array

1.3 Solar Cell Conversion Efficiency

For a traditional solar cell, conversion efficiency is defined as the ratio of the greatest power output generated to the power input, or incident power. The following output properties, which are defined, have a big impact on a solar cell's efficiency.

1.3.1 Short Circuit Current (Isc)

When the solar cell's electrodes are damaged, the short circuit current (Isc), which travels through the external circuit, occurs. Both the flux density and the spectrum of the incident light have an impact on this current. The AM1.5 wavelength is used as the reference spectrum for measurements of typical solar cell parameters [9]. At any given light level, this is the solar cell's maximum current delivery capacity. The highest wavelength at which a specific semiconductor may produce electron-hole pairs is the highest wavelength at which the maximum I_{SC} is calculated. The equation E (eV) = 1.24 is frequently used to explain the connection between the 1.1 eV band gap. When exposed to an AM1.5 spectrum, crystalline silicon solar cells have a maximum output of 46 mA/cm^2 [10].

1.3.2 Open-Circuit Voltage (Voc)

The voltage is referred to as the "open-circuit voltage" when the solar cell terminals are open or disconnected from a load because no current is currently flowing through the external circuit at that time. It is the highest voltage a solar cell is capable of producing under any particular illumination situation [11]. In this equation, the photo-generated current density I_{photon}, the saturation current I_S, and the voltage V_{OC} are all connected. The open circuit voltage, which largely depends on the saturation current, is another sign of recombination in the solar cell. The maximum value of the open circuit voltage for silicon solar cells is 700 mV [12].

1.4 Objectives of the Project

The objectives of the project are to compare the output power in the system when there is a fault in the PV such as; line-line fault, open circuit fault and ground faults.

1.5 Expected Outcomes

The goal of this project is to evaluate and compare the power output under normal and fault conditions. The results will be generated from the simulation of the specification data.

1.6 Project outline

Chapter 1 introduces the overall aspects of photovoltaic (PV) systems. The background details of solar cells, modules, and arrays are presented.

Chapter 2 includes the literature review on faults in a PV array, Fault-Tolerant PV system, reconfigurable PV panel and the classification of faults in PV arrays.

Chapter 3 compiles the modeling and simulations of PV modules

Chapter 4 includes results and analysis of PV module and array.

Chapter 5 contains the future scope and conclusion of this project.

Chapter 2

Faults in a PV Array

2.1 PV Cell Faults

Numerous factors including contact failure, wire corrosion, hail damage, moisture, etc., can cause a PV system to malfunction [13]. In a two-year monitoring study of 27 PV systems, the authors [14] found that the annual occurrence rates of PV cell failures ranged from 1.1% to 11.7%. The failure rate of PV systems in space is significantly higher as a result of the rise in orbital debris [15]. An open circuit at the PV cell position is the same as a PV cell fault. The remaining PV cells in the same PV cell group experience a reverse bias when one PV cell fails. The reverse bias issue can be solved by integrating bypass diodes with PV cells [16, 17]. Figure 3.1 shows a typical PV system architecture. A single bad PV cell would reduce output power by 1/16, or 6.25%, for the PV panel. Because PV cells in a PV panel cannot function at their MPPs when the balanced structure of a PV panel is harmed by the faults, the true output power loss caused by one defective PV cell is 16.5% [28].

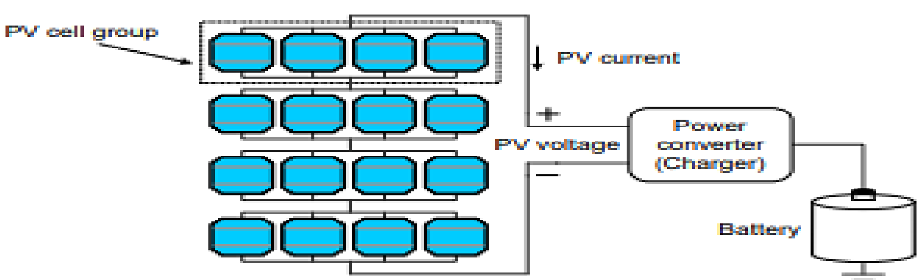

Figure 2.1 A typical PV system architecture [27]

Unfortunately, manually identifying and resolving problems with distant PV systems (e.g. PV systems in orbital or deep space missions) are both costly and technically difficult. It is essential to design a PV system that can withstand failures in order to enable an embedded system controller to dynamically address PV cell problems.

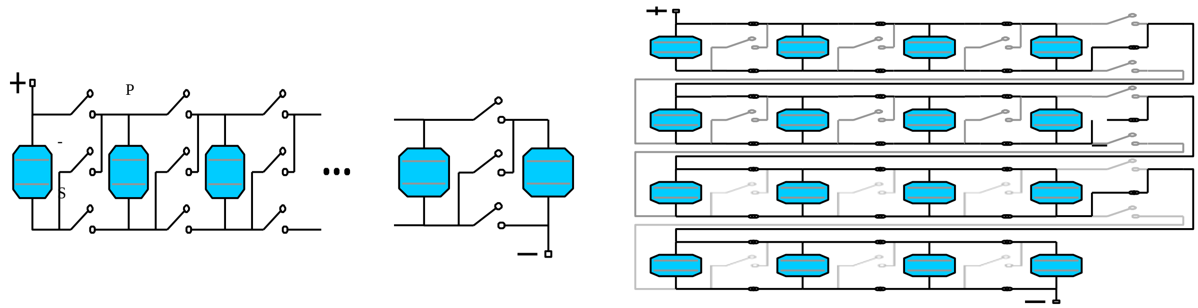

(a) (b)

Figure 2.2 (a) PV panel construction (b) Configuration of a PV panel [27]

2.2 Fault- Tolerant PV systems

Fault-tolerant technologies are preferred for PV systems to last longer. Several methods for diagnosing PV cell faults have been put forth [18 - 20]. These methods can identify defects in PV cells; however, they lack an efficient fault bypassing mechanism, cannot find problems on the panel, or require additional equipment (such as signal generators) for fault diagnostics [21, 22]. This is not surprising given that these methods for problem identification are typically limited by the fixed (non-programmable) structure of the PV panel.

2.3 Reconfigurable PV Panel

A fault-tolerant PV system was designed in [22, 23] using the reconfigurable PV panel topology shown in Figure 2.2(a). By using unbalanced PV cell connection topologies within the PV panel, this construction for a PV panel was first proposed by [24] to combat the partial shadowing effect. In this research, we suggest using the same reconfigurable PV panel topology for defect bypassing and failure detection [25]. The suggested reconfigurable PV panel is built with each PV cell combined with two P-switches and one S-switch, with the exception of the final one. Figure 2.2(a) depicts the electrical connectivity between the switches and PV cells. [24, 25]. We can configure the PV panels for typical system functioning by adjusting the ON/OFF states of the switches. How to obtain the 4 × 4 structure seen in Figure 2.2(a) is shown in Figure 2.2(b). The PV panel is constructed in such a way that, for typical system operation, the output voltage of the panel at its MPP matches the battery voltage. The charger increases the output power of the PV system while utilizing the least amount of energy possible. However, aging, partial shadowing, and temperature variations can all affect a PV cell's MPP voltage. In these circumstances, we can move the PV panel to increase the PV system's output power [22]. We could convert a (4 × 4) setup into a (8 × 1) one, for instance. This adaptability allows PV systems to operate more effectively in a variety of environmental circumstances.

2.4 Reconfiguration for Fault Detection and Fault Bypassing

Defect detection seeks to identify any PV cell problems in the PV panel. Bypassing faults tries to modify the structure of the PV panel to reduce output power loss brought on by faulty PV cells. Imagine a PV panel with a (N × M) configuration under ideal conditions [26]. We may need to build a (r × M) PV panel configuration (r ≤ N) using a particular combination of PV cells in order to determine the combined output power of those cells if there is a PV cell issue in this area of the PV panel. To increase the system output power during fault bypassing, we might need to build a $N_{opt} \times M_{opt}$ PV panel arrangement ($N_{opt} \times M_{opt} \leq N \times M$) in which the failed PV cells and perhaps some healthy PV cells are omitted [27, 28].

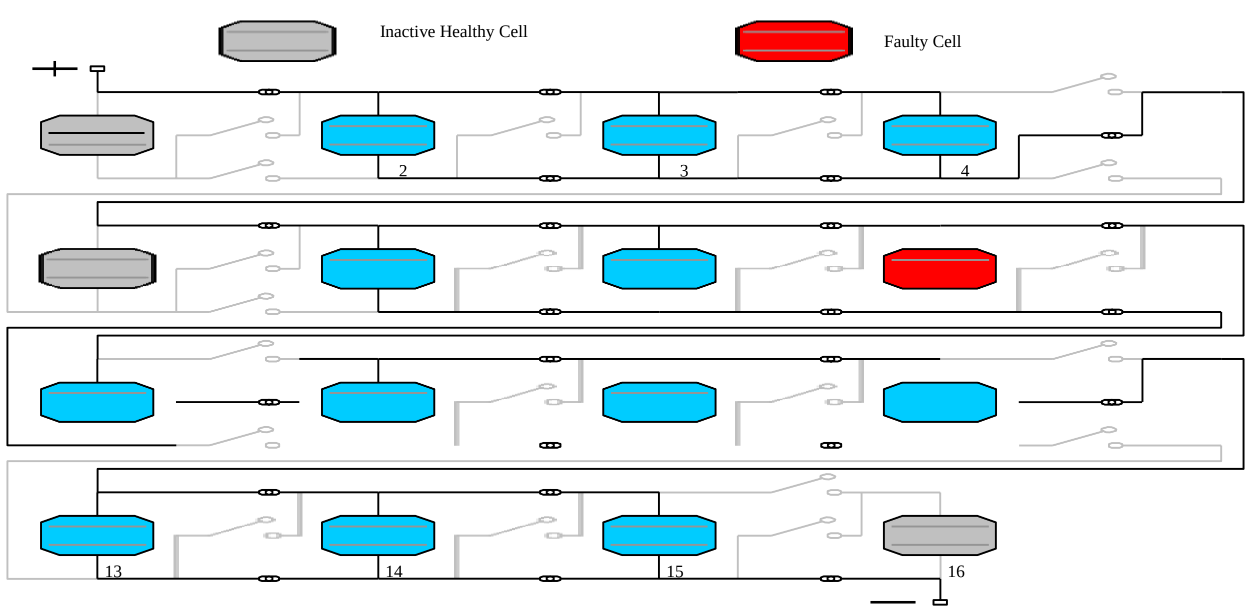

Figure 2.3. Example of PV panel reconfiguration during fault Detection and bypassing [28].

It could be necessary to shut down even healthy PV cells in certain fault bypass situations. Taking into account the case where we have 42 PV cells and one of them is broken. We are unable to assemble a stable setup where the battery voltage and MPP voltage match with a prime number of 41 healthy PV cells. Therefore, in order to have 40 active PV cells, we would like to deactivate one healthy PV cell [28]. Thus, by arranging the PV system in a 5×8 or 8×5 configuration, the output power can be increased. If we meet another PV cell problem, we could employ the active PV cell that was previously inactive. In order to correctly control the ON/OFF states of the switches for fault detection and fault bypassing in this project [25, 26], we will use Figure 2.3 as an example. The aim of this project is to examine the fault.

2.5 Classification of Faults in PV Array

The following section includes the explanation of fault classification for this project.

2.5.1 Faults in PV Array

The two primary types of PV array defects are cabling and PV panel faults. The most frequent types of defects in PV panels and modules include earth faults, bridge faults, open circuit faults, and mismatch faults.

2.5.2 Ground Fault

When the circuit accidentally creates a path to the ground, a ground fault occurs. PV systems must contain two different forms of grounding: system grounding and equipment grounding. When the system is grounded, Ground Fault Prevention Device (GFPD) in the PV inverter grounds the negative conductor. Equipment grounding should be used to ground the exposed non-current-carrying metal components of conductor enclosures, electrical equipment, and PV module frames [20]. Lower Ground Fault and Upper Ground Fault are the two types of ground faults that might arise [19, 20].

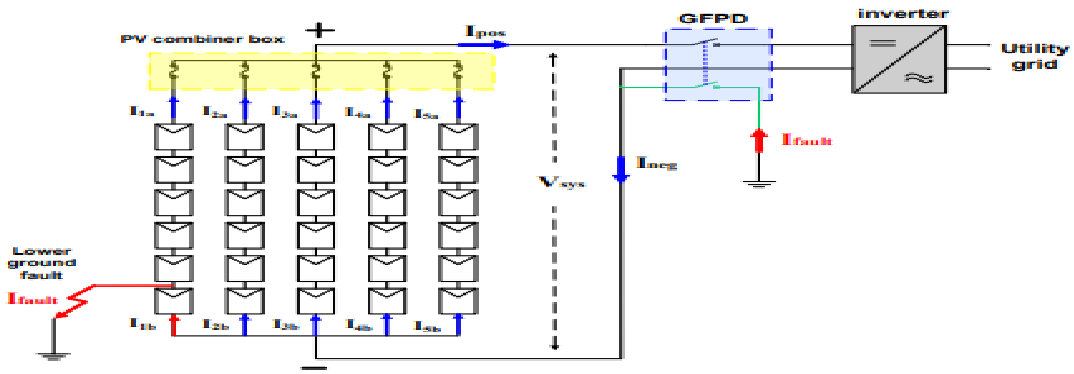

Figure 2.4 Schematic diagram of a lower ground fault under STC

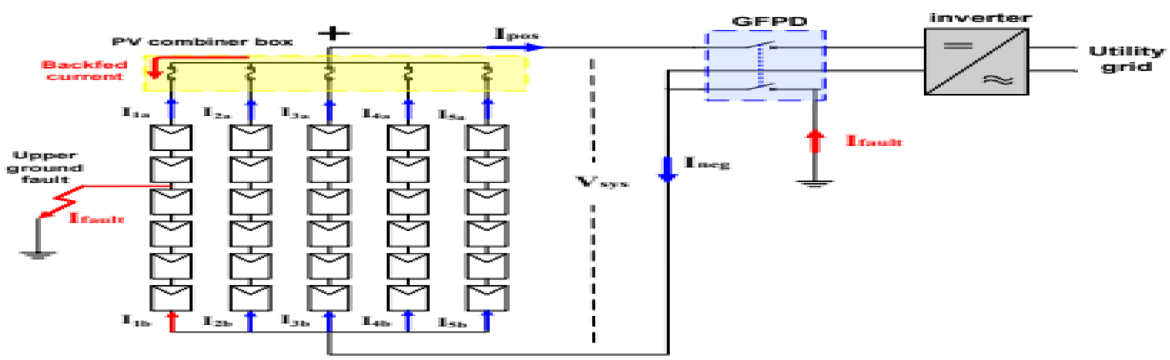

Figure 2.5 Schematic diagram of upper ground fault under STC

2.5.3 Open Circuit Fault

An open circuit failure happens when one of the current-carrying routes in series with the load is compromised or broken. Incorrect connections between cells, plugged-in and unplugged connectors at junction boxes, or wire breaks can cause these failures [16].

2.5.4 Line-Line Fault

A line-line fault is an unintended low-resistance connection made between two electrically charged sites in a system or network. A line-line fault in PV systems is typically described as a short-circuit fault between PV modules or array wires of different potentials. Line-line faults are assumed in this study to not involve any ground points. Without any ground points, a line-line fault might be classified as a ground fault [26].

Chapter 3

Modeling and Simulation of PV Modules

3.1 Solar Cell Models

It is not suitable to simply model solar cells as a constant voltage source or a constant current source due to their non-linear I-V properties. The two models that are most frequently used to describe the electrical behaviors of solar cells are the one-diode model and the double-diode model [26, 27]. Figures 3.1(a) and 3.1(b), which represent the analogous circuits for the one-diode and double-diode models, respectively.

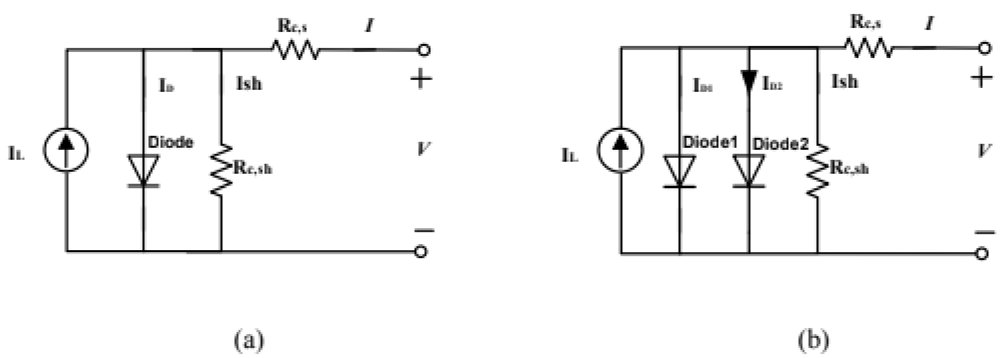

Figure 3.1 Equivalent circuits for (a) the one-diode model and (b) The double-diode model

The solar cell current equation is shown below and it is applicable to the one-diode model in Fig. 3.1(a).

$$I = (I_L \; - \; I_D \; - \; I_{sh}) \tag{3.1}$$

$$I = I_L \text{-} \; I_S \left[\exp\left(\frac{V+IR_{c,s}}{AkT} \; .q\right) - 1\right] - \frac{V+IR_{c,s}}{R_{c,sh}} \tag{3.2}$$

where

I = solar cell current (A), V = solar cell voltage (V), I_L = light-generated current (A), I_D = diode current (A), I_{sh} = shunt resistance current (A) and I_S = saturation current of the diode (A).

Also,

R c, s = solar cell series resistance (ohms), Rc, sh = solar cell shunt resistance (ohms), q = electron charge = 1.6×10-19 C, k = Boltzmann's constant = 1.38×10-23 J/K, A = diode ideal factor (1 ≤ A ≤ 2), and T = ambient temperature (K).

The equation for the solar cell current in the double-diode model is:

$$I = (I_L - I_{D1} - I_{D2} - I_{sh}) \tag{3.3}$$

$$I = I_L \text{-} I_{S1}\left[\exp\left(\frac{V+IR_{c,s}}{kT}\,.\,q\right)-1\right] - I_{S2}\left[\exp\left(\frac{V+IRc,s}{2kT}\,.\,q\right)-1\right] - \frac{V+IR_{c,s}}{R_{c,s}} \tag{3.4}$$

where

I_{S1} = saturation current for diode1 (A), I_{S2} = saturation current for diode2 (A), I_{D1} = diode1 current (A), and I_{D2} = diode 2 current (A).

The one-diode model is used in this project instead of the double-diode model since it has a number of advantages over the latter:

- The numerical method for the one-diode model converges faster than the one of the double-diode model in the simulation environment;
- The detailed parameters of the one-diode model are available for the majority of PV modules on the market.
- The one-diode model is accurate enough for steady-state and fault analysis for PV modules at the system level [28].

3.2 Modeling Algorithm

It is unrealistic to model each solar cell in a PV array while modeling it. Additionally, rather than bulk solar cells, PV manufacturers typically only offer finished, environmentally safe modules to end customers. Additionally, solar cells manufactured in the same module typically experience almost identical irradiance circumstances in real-world working conditions. For these reasons, we may only assume that each PV module's solar cells have the same properties and operating conditions. As a result, a PV module can be thought of as a fundamental component made up of identical solar cells. As a result, the modeling and simulation of PV modules become crucial phases in the normal and fault analysis of PV systems. The following is the development of the PV module simulation model. The modeling program solves (3.1) iteratively to get the mathematical solution for (I_L-I_D), and then feeds the result to a regulated current source in Fig. 3.2(a), which represents a one-diode PV module model shown in Fig. 3.2(b).

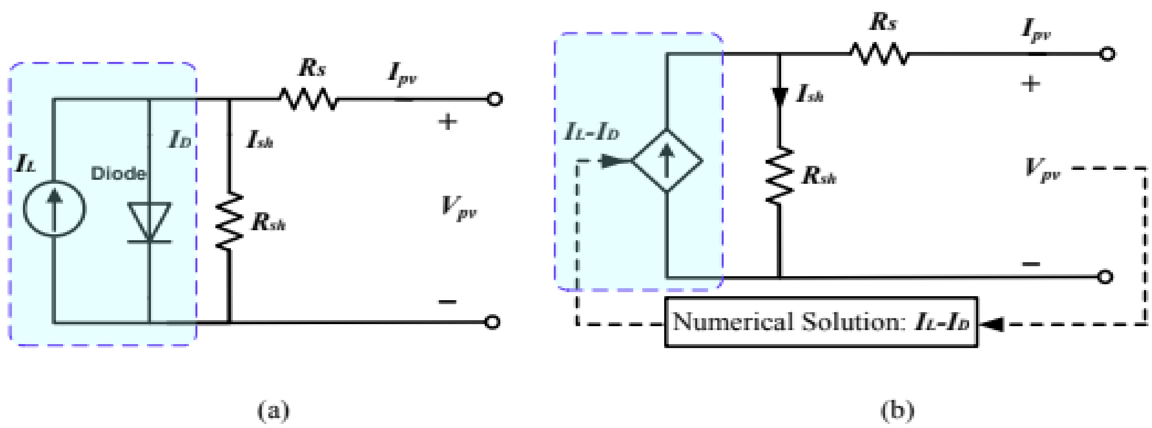

Figure 3.2 One-diode model for a PV module (a) equivalent circuit and

(b) Numerical model

The model for a PV module, which was created from the one-diode model, is written as [28]:

$$I = I_L - I_S\left[\exp\left(\frac{V_{pv}+I_{pv}\times R_S}{AkT\times N_S}\;q\right)-1\right]-\frac{V_{pv}+I_{pv}\times R_S}{R_{sh}} \tag{3.5}$$

where

Ns = the number of solar cells in series for a PV module

I_{pv} = PV module current, V_{pv} = PV module voltage

R_S = PV module series resistance and R_{Sh} = PV module shunt resistance.

The light produced by current I_L varies depending on sun irradiation and surrounding temperature and is characterized as:

$$I_L = \frac{G}{G_0}[I_{L0} + C_T (T - T_0)] \qquad (3.6)$$

where

G = solar irradiance (W/m^2), G_0 = reference solar irradiance (W/m^2), I_{L0} = reference light generated current (A), T_0 = reference temperature (K), and C_T = temperature coefficient of the light generated current (A/K) [27].

The saturation current I_S of the diode varies with temperature and is as follows:

$$I_S = I_{S0} \times \left(\frac{T}{T_0}\right)^3 exp\left[\frac{q \, . \, E_g}{Ak} \, . \left(\frac{1}{T_0} - \frac{1}{T}\right)\right] \qquad (3.7)$$

For Si, the band gap energy (E_g) is temperature dependent and can be expressed as follows:

$$E_g = 1.170 - \frac{4.73 \times 10^{-4} \, T^2}{T + 636} \, eV \qquad (3.8)$$

where

E_g = Band gap energy of the material (eV), and 1 (eV) = 1.6×10-19 J.

E_g, may have a range of values depending on the semiconductor material used in PV modules. Under normal room temperature conditions, E_g is typically in the range of 1.12 eV for crystalline silicon, 1.03 eV for copper indium selenide (CIS), 1.7 eV for amorphous silicon, and 1.5 eV for cadmium telluride (CdTe).

3.3 Simulations of PV Modules

The suggested numerical model (shown in Fig. 3.2(b)) can be accurately simulated in MATLAB/Simulink and in any circuit simulation software (such as PSpice). Since MATLAB/Simulink contains the SimPowerSystems toolbox, which may provide an open and flexible interface to model numerical, electrical, and control systems, it was chosen for this project as the simulation environment.

Fig. 3.3 depicts the numerical model for PV modules as an example. There are three inputs to the "Numerical Solution" subsystem: irradiance, temperature, and the terminal voltage Vpv of a PV module. The model for PV modules in MATLAB/Simulink is shown in Fig. 3.4, where a Simulink subsystem is employed as the "Numerical Solution" block. Voltage measuring block, regulated current source, and series RLC branch make up the remaining parts.

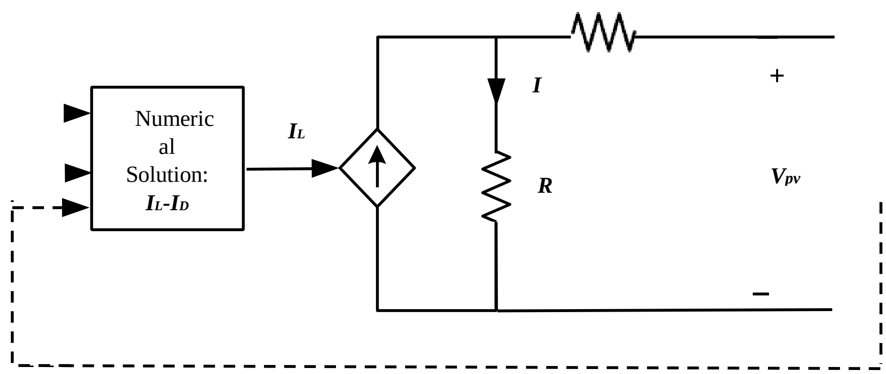

Figure 3.3 Numerical model for PV modules

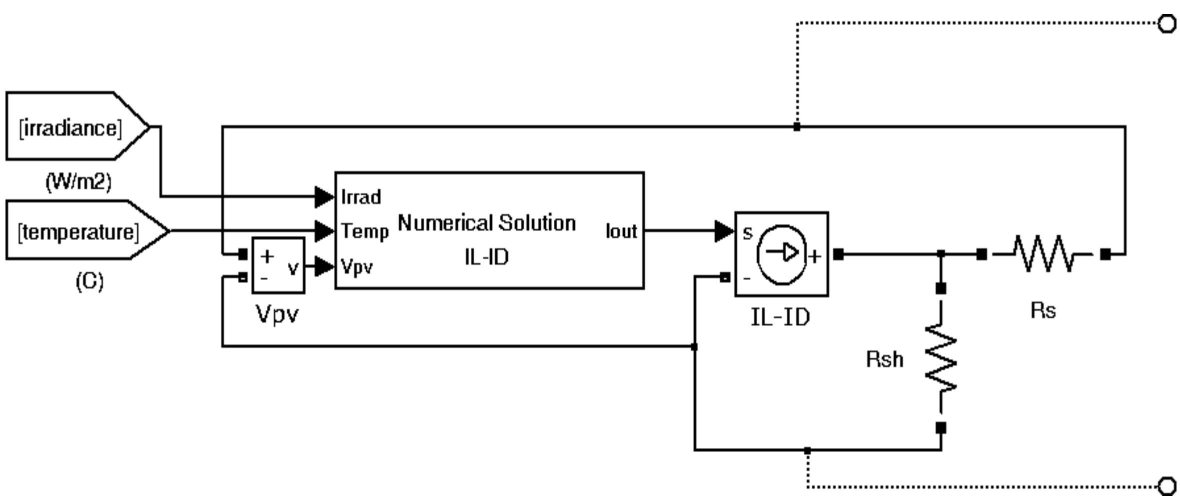

Figure 3.4 Simulation model for PV modules in MATLAB/Simulink

All of the constant parameters for PV modules are set in InitFcn of Callbacks in the Model Properties menu of Simulink in order to initialize the simulation. By choosing Look under Mask from the Numerical Solution menu of the subsystem, as illustrated in Fig. 3.5, function blocks for the numerical solution (I_L-I_D) can be changed. A crucial part of this subsystem's search for the numerical solution is played by a function block called Algebraic Constraint. The block outputs the diode voltage V_D, which impacts the input through the feedback loop and inescapably constraints input at zero. The input signal is limited to

$$I_L - \left(I_{pv} + I_D + I_{sh}\right) = 0 \tag{3.9}$$

The input windows for the model, as shown in Fig. 3.6, allow the major parameters for PV modules, including Isc, I_{SO}, Voc, C_T, and A to be specified as constants. This makes the MATLAB/Simulink model a potent toolkit for study and design of PV systems because it means the model may be universal and applicable to any PV modules in the solar industry.

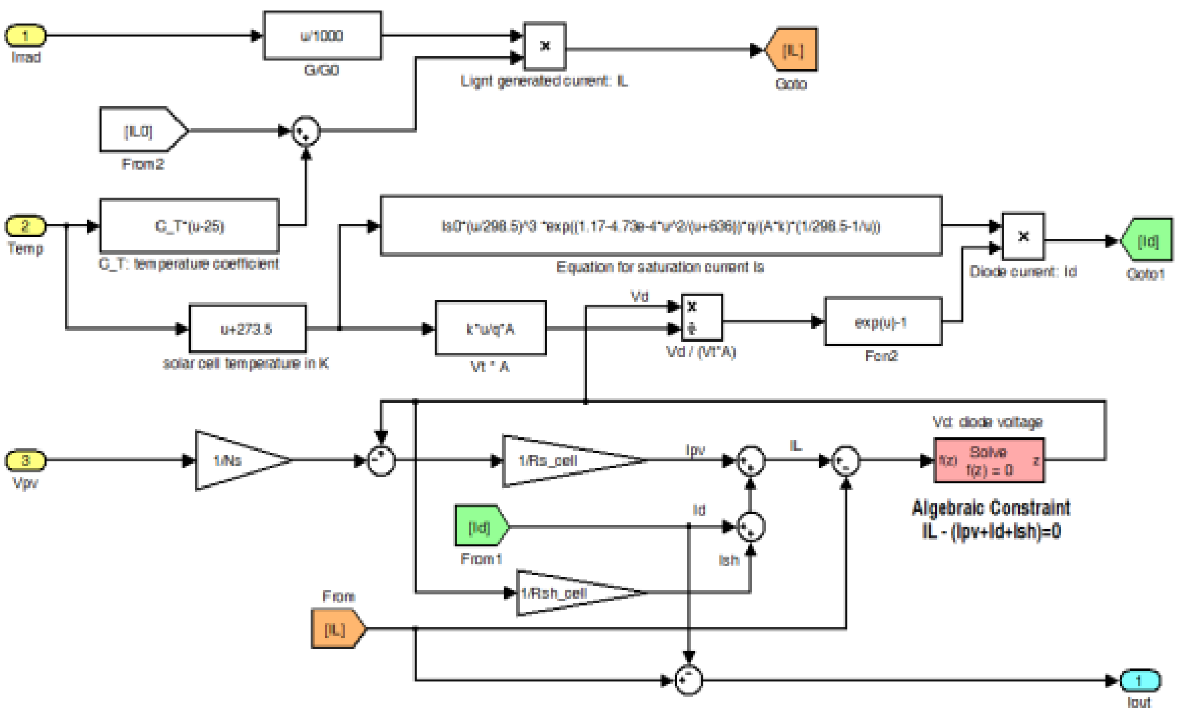

Figure 3.5 Numerical solution of subsystem in MATLAB/Simulink

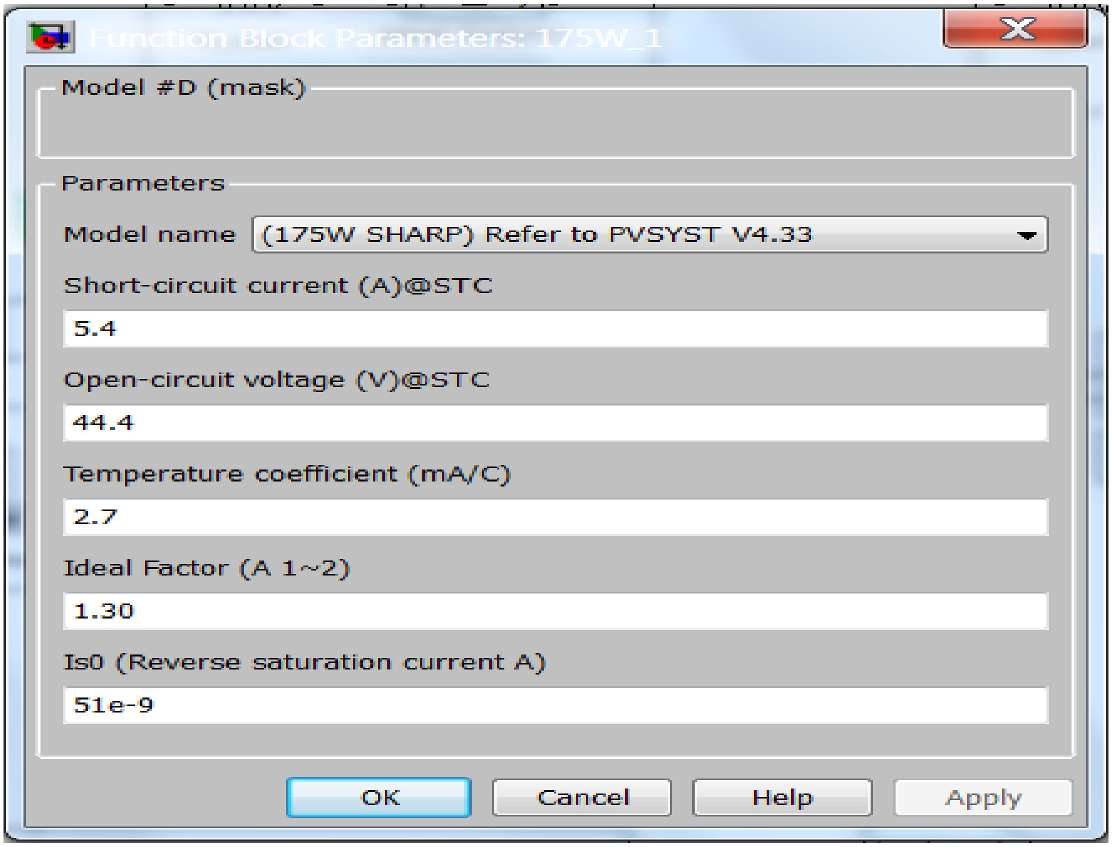

Figure 3.6 Primary input Parameters for PV module in MATLAB/Simulink

Chapter 4

Results and Analysis

4.1 I-V Characteristics of PV Cell

I-V characteristics is a fundamental tool for normal and fault condition analysis and defines the behavior of PV arrays. The normal part and the faulted component of a series-parallel configured PV array operates at the same voltage as indicated in Fig. 4.1. It is possible to determine the operating points of both the normal and defective portions of the array using the PV arrays' provided I-V characteristics and array operation voltage. Using the simulation model shown in Fig. 3.4, the PV system is created in MATLAB/Simulink. Each PV model in simulations depicts a modular, scalable PV module.

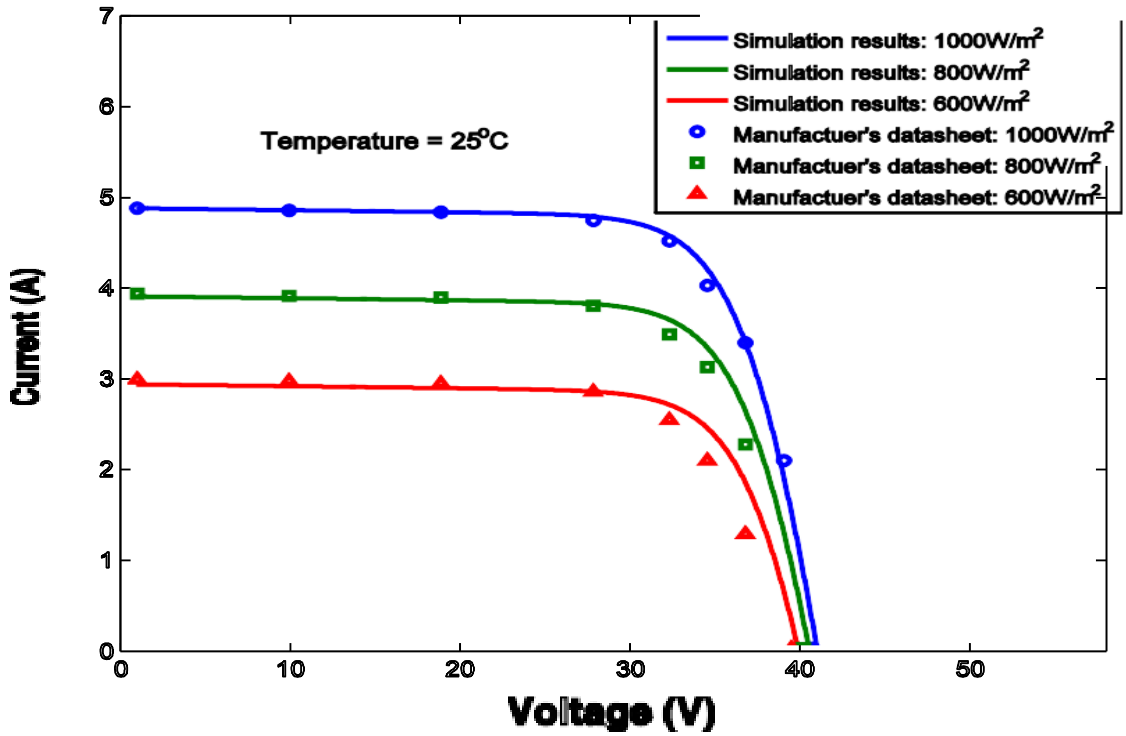

Figure 4.1 I-V curves of simulation model

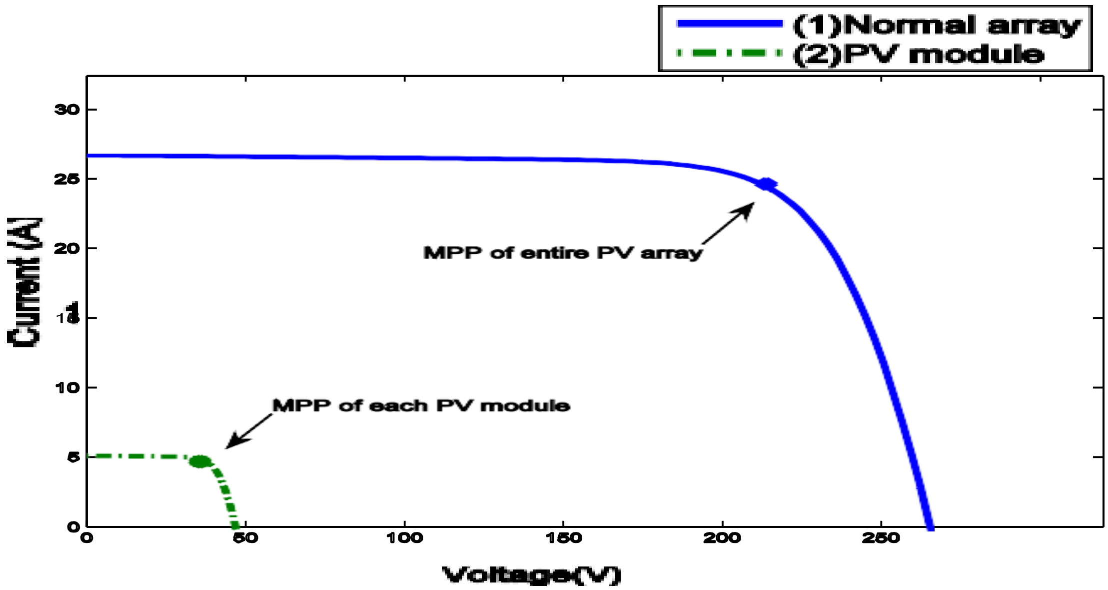

Figure 4.2 I-V curves of PV array and PV module at STC

4.2 Lower Ground Fault

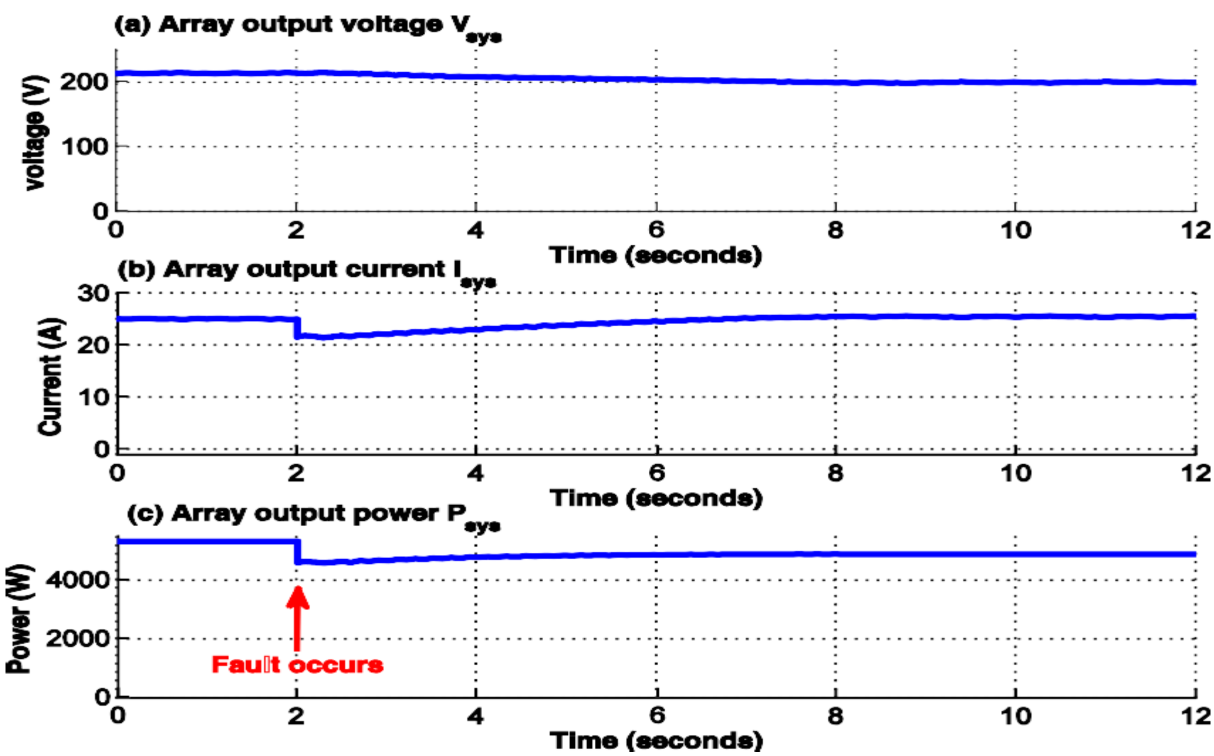

Figure 4.3 Simulated results of the entire PV array under a lower ground fault at STC

A lower ground fault with zero fault impedance happens between the final two modules at PV String #1, as depicted in Fig. 4.4. Voltage fluctuations and imbalanced currents between the damaged string and other healthy strings are frequent effects of the instantaneous fault.

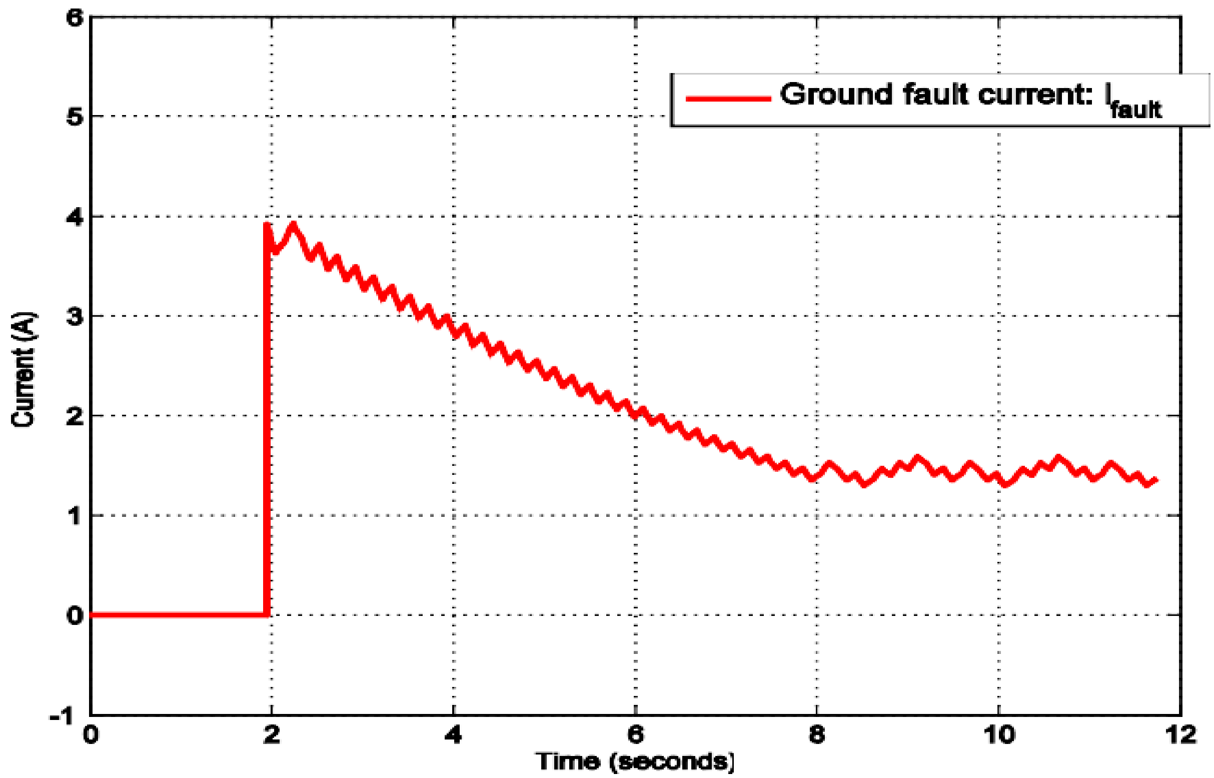

Figure 4.4 Simulated fault current (I_{fault}) of a lower ground fault under STC

The ground-fault current I_{fault} has a maximum magnitude of 3.92A when the ground fault happens at time t=2s (0.726Isc). The MPPT then notices the abrupt shift in output power and starts reducing I_{fault} to 1.4A. (0.26Isc). the faulty string current is raised by the MPPT from 1.5A (0.28Isc) to 3.95A (0.73Isc). There is no back feed current flowing into the affected string in this lower ground fault scenario. The ground-fault current is more than 0.5A, allowing the GFPD to trip it.

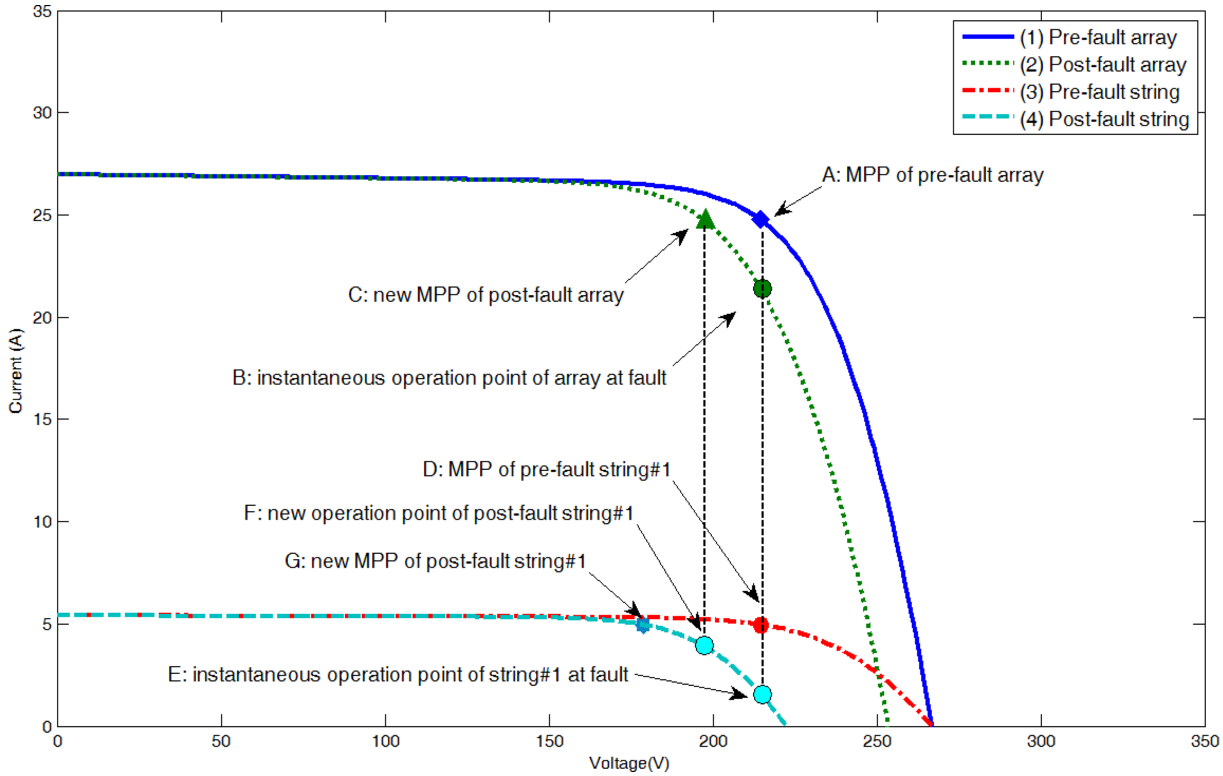

Figure 4.5 I-V characteristics of PV array under lower ground fault

4.3 Upper Ground Fault

This upper ground fault will cause large back feed current and very high ground-fault current. Fig. 4.6 shows that the ground-fault current I_{fault} reaches its greatest magnitude of 27.22A after the ground fault occurs at time t=2s (5.04Isc). The String #1 is simultaneously receiving a significant quantity of back feed current, 21.75A (-4.03Isc), from other typical strings. The ground-fault current in this instance is greater than 0.5A and can trip the GFPD (not included in simulation). The negative current-carrying conductor of the array is no longer grounded when the ground fault is cleared by the GFPD, disconnecting the fault line. The linked switches in the GFPD also instantly open the positive wire.

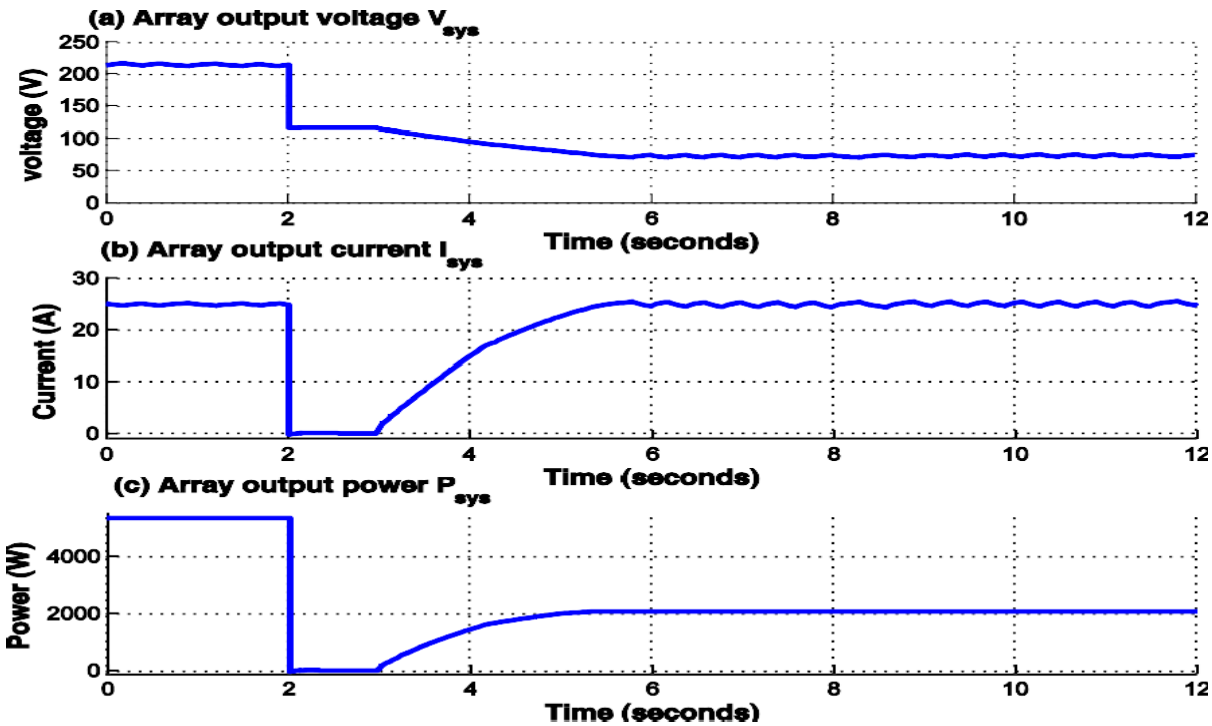

Figure 4.6 Simulated results of entire PV array under upper ground fault

The output voltage (V_{sys}), current (I_{sys}) and power (P_{sys}) of the entire PV array are illustrated in Fig Fig. 4.6.

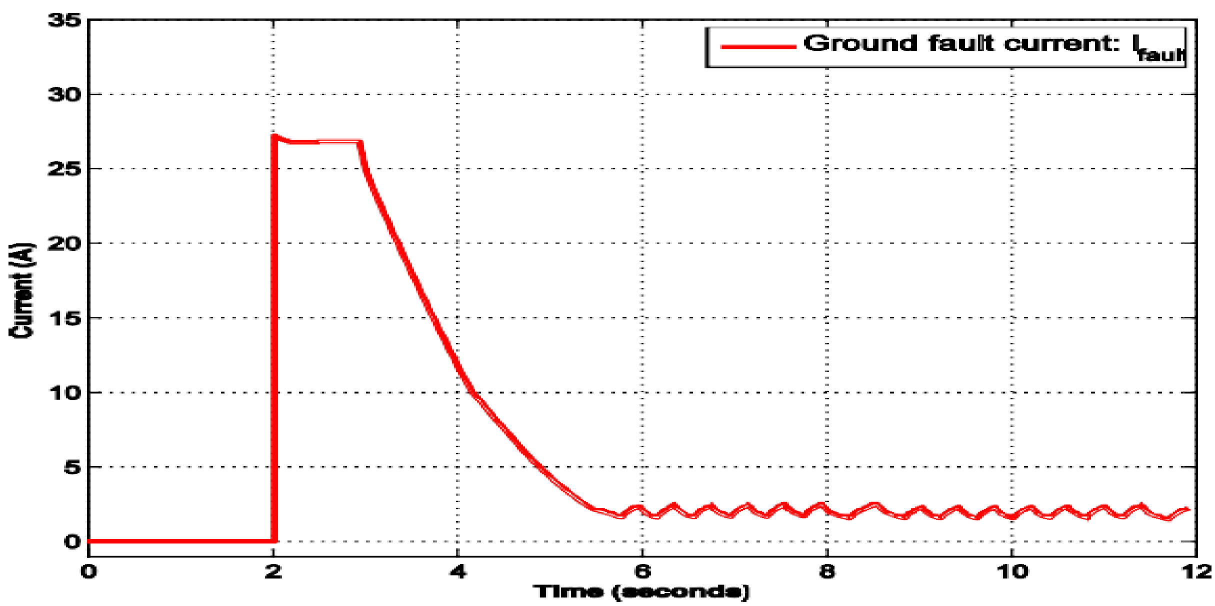

Figure 4.7 Simulated fault current (I_{fault}) of upper ground fault under STC

4.4 Line-Line Faults in a PV Array with Small Voltage Difference

A line-line fault is an unintended low-resistance connection made between two electrically charged sites in a system or network. A line-line fault in PV systems is typically described as a short-circuit fault between PV modules or array wires of different potentials. Line-line faults are assumed in this study to not involve any ground points. Without any ground points, a line-line fault might be classified as a ground fault.

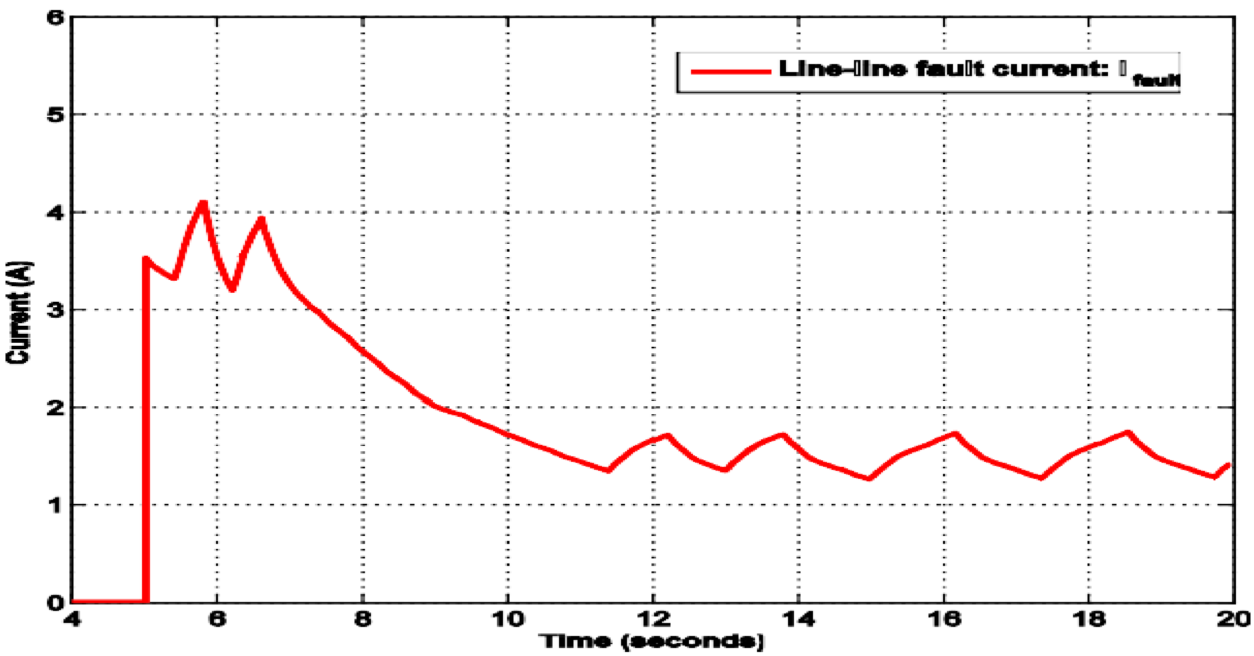

Figure 4.8 Simulated fault current (I_{fault}) of a line-line fault with Small Voltage difference

After the line-line fault occurs, the fault current I_{fault} has reached its maximum magnitude (4A) shown above in fig. 4.8 and decreases to around 1.5A (0.28I_{sc}) with the help of the MPPT. The top current of the malfunctioning String #1 first reaches its minimum value of 1.75A (0.32Isc) before being increased to 3.7A (0.69Isc) by the MPPT. There is no back feed current into the faulty string in this instance, and no overcurrent exceeds the fuses rated current of 5.4A. (1.56Isc). As a result, line-line faults with low voltage differences cannot trip traditional protection mechanisms. This line-line problem could be permanently concealed in the PV array, reducing system efficiency and reliability.

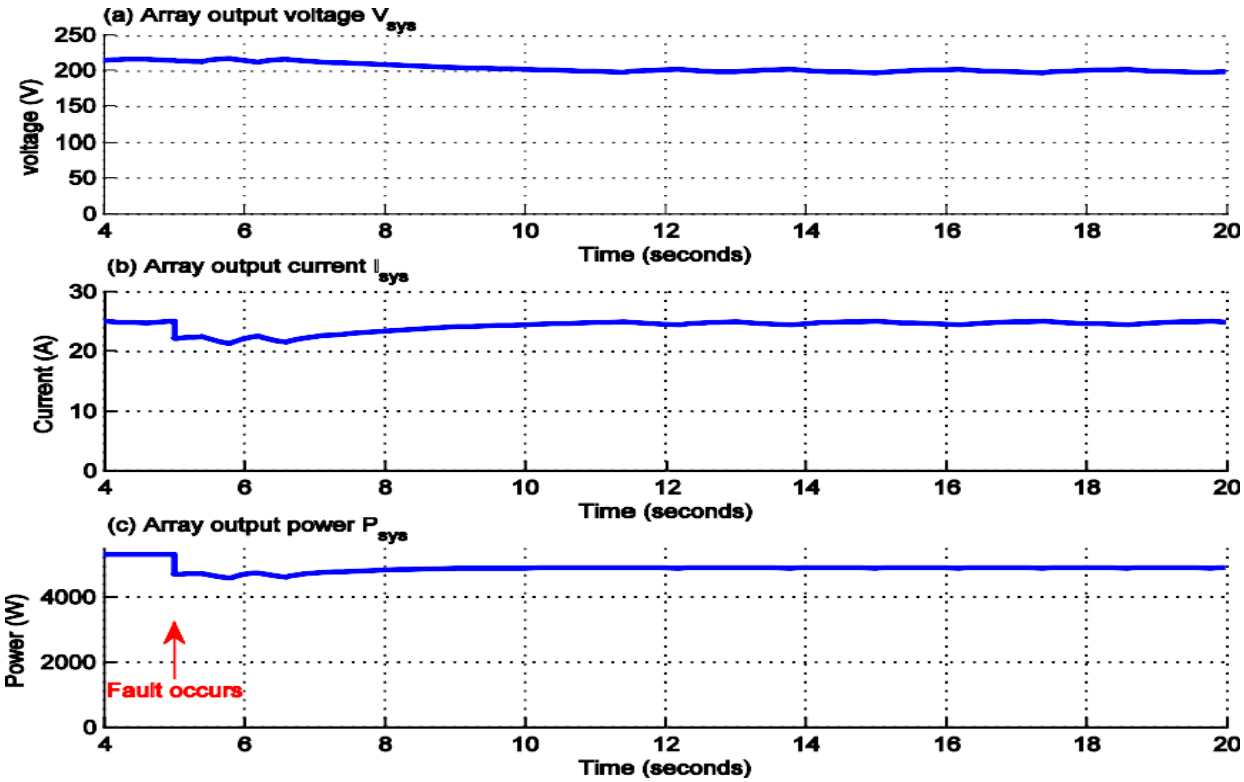

Figure 4.9 Simulated results of entire PV array under a line-line fault with small voltage difference

4.5 Line-Line Faults in a PV Array with Large Voltage Difference

When a line-line fault occurs as shown in fig. 4.10, the fault current I_{fault} reaches its maximum value (19.8A), at which point it uses the MPPT to reduce to about 2A. The highest current of the malfunctioning String #1 first hits its negative minimum of 13A (-2.4Isc) before being increased to 3.3A (0.61Isc) by the MPPT. Due to the faulty String #1's enormous back feed current, the fuse safeguards will melt in this situation (rated no less than 1.56Isc). Therefore, traditional protection devices will effectively clear the line-line fault under STC with a significant voltage difference.

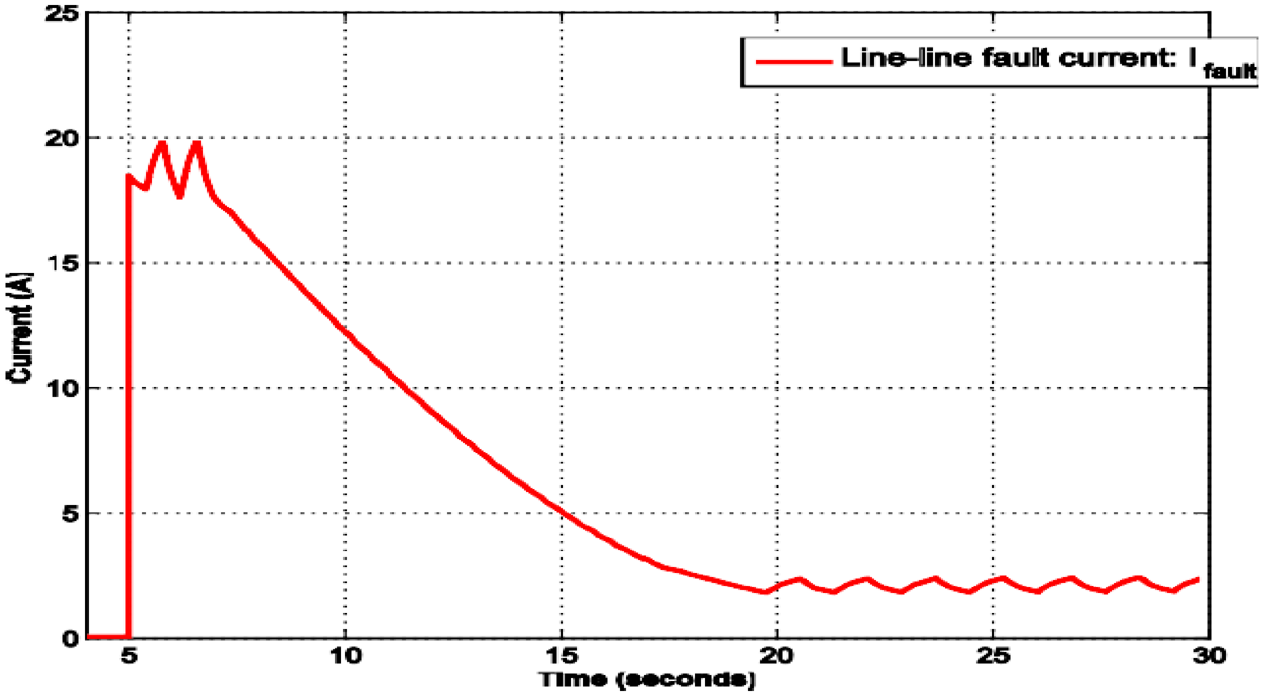

Figure 4.10 Simulated fault current of a line-line fault with large voltage difference

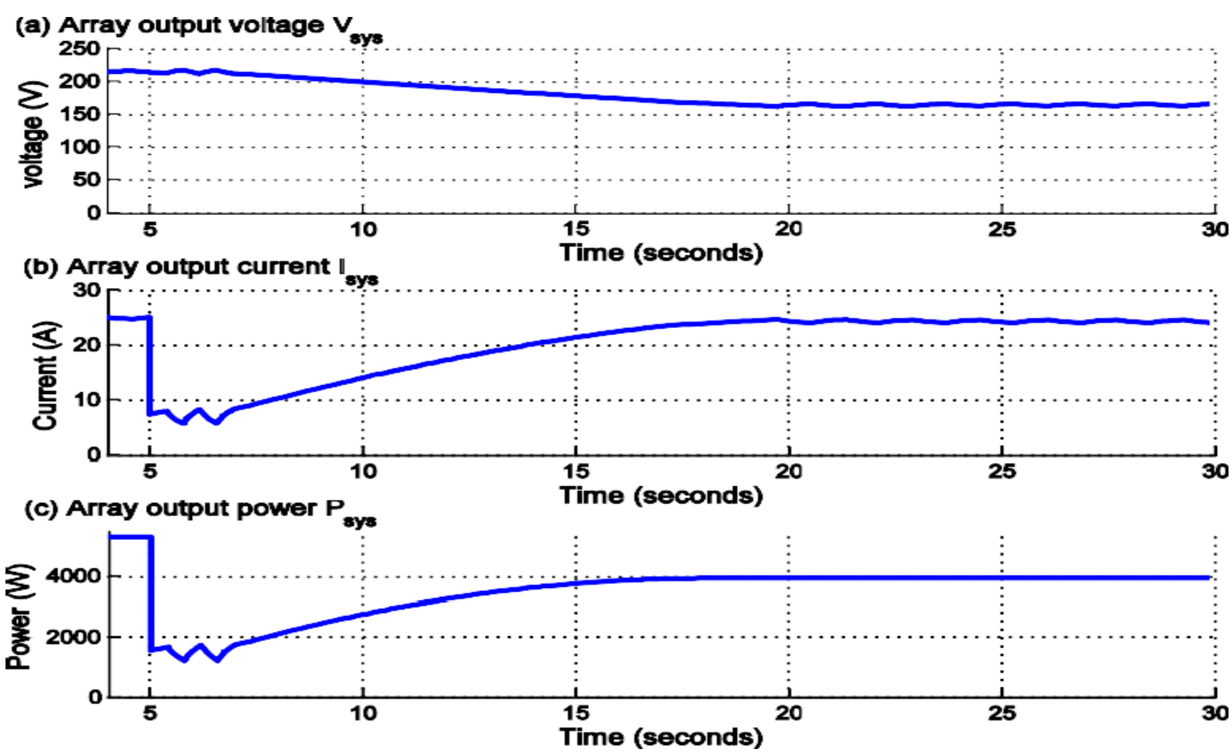

Figure 4.11 Simulated results of entire PV array under a line-line fault with large voltage difference

4.6 Open-Circuit Fault in a PV Array

An open-circuit fault is an accidental disconnection at a normal current-carrying conductor. For example, there is an open-circuit fault at point "*F*" on the String #1 of a PV array (see Fig. 4.12). This fault might occur on cracking PV cells/modules, or between module interconnections, typically in bus wiring or junction box.

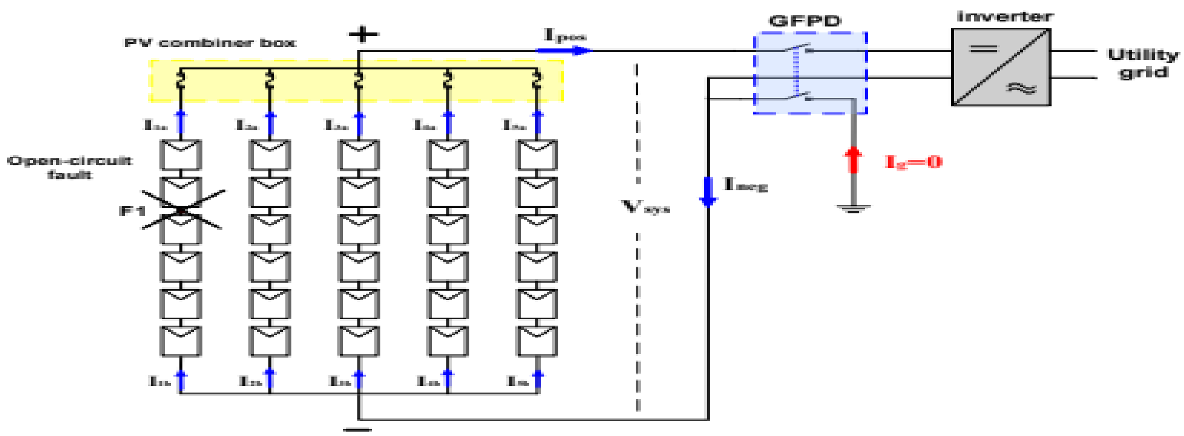

Figure 4.12 Schematic diagram of an open-circuit fault in PV array

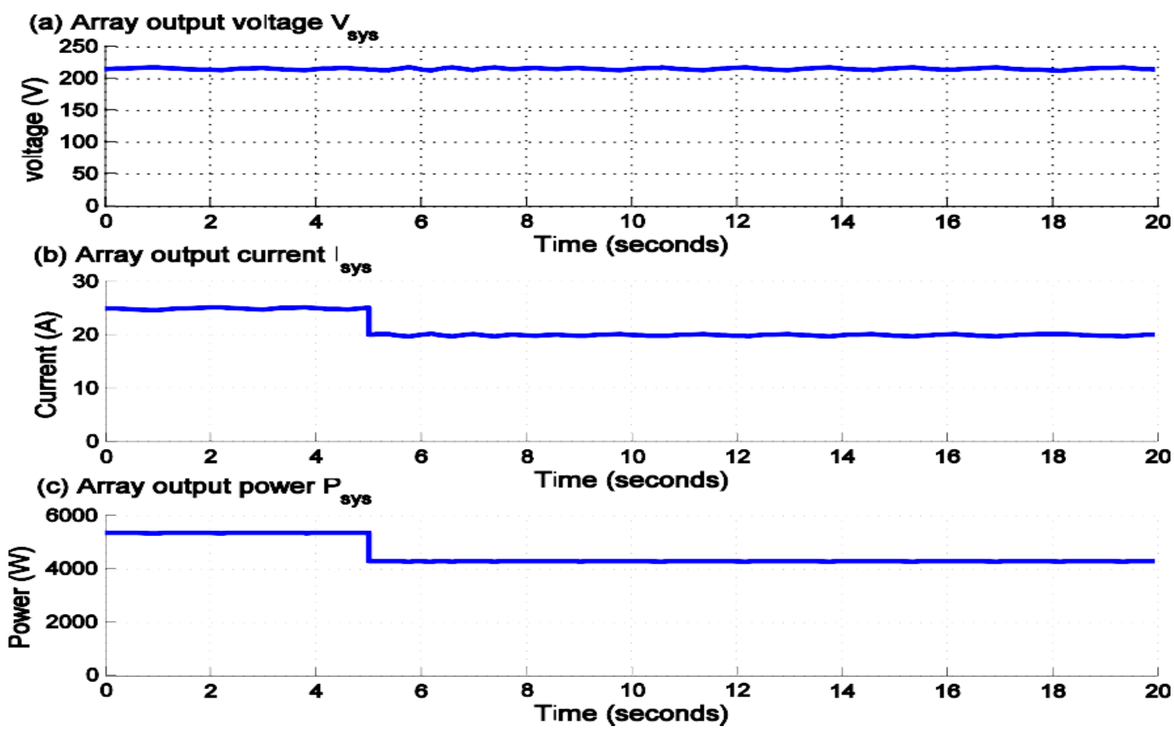

Figure 4.13 Simulated results of entire PV array under an open-circuit fault

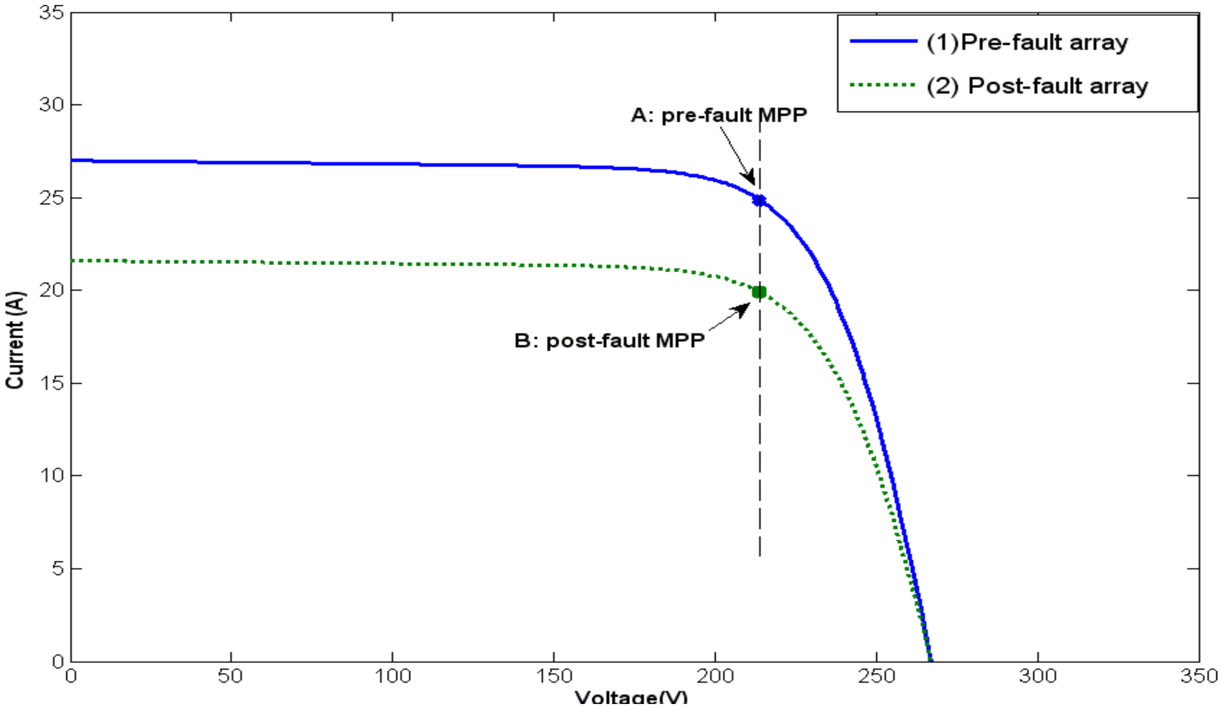

Figure 4.14 I-V characteristics of PV array of an Open-circuit fault

The open-circuit defect in the PV array is described in more depth by the I-V curve analysis in Fig. 4.14. Pre-fault and post-fault MPPs are also present. The PV array is operating normally at its rated MPP "A" prior to the fault. The current of String #1 (I1a) decreases to zero right away after the open-circuit fault occurs at time t=5 s because String #1 is cut off as a result of the fault. The PV array is left with 4 functioning strings as a result, and its operation point unexpectedly changes to point "B" from the pre-fault MPP "A." And the MPP of the post-fault array happens to be at point "B." The remaining PV strings will operate at their post-fault optimum at 80% of total rated power with the aid of the inverter's MPPT. Open-circuit faults in PV arrays do not result in overcurrent generation, in contrast to ground faults or line-line failures. The open-circuit fault, which often involves reduced array system current (I_{sys}) but almost the same array system voltage (V_{sys}) as the typical PV array voltage, will instead cause significant power loss.

Chapter 5

Conclusion and Future Scope

5.1 Conclusion

The findings of our investigation show that fault current in PV arrays varies significantly on the PV array's irradiance level in addition to fault sites. It has been shown that even the same defect in a PV array might result in different fault currents under high and low irradiance. The PV array's irradiance and voltage gradually decrease as dusk approaches. The inverter shuts down and the MPPT stops when the PV array voltage cannot support the inverter's minimal operational voltage. The PV array switches to open circuit and produces no power in the meantime. Because of this, the currents in normal PV strings can only back feed into the faulty string. As a result, when the inverter shuts off, the I_{back} rises to its negative high of -0.17A (-0.29Isc). I_{back}, however, is never high enough to trip a fuse (usually rated at 1.56Isc). I_{back} equals 0 as time passes and irradiance approaches zero. The modeling approach is successfully implemented in MATLAB/Simulink and converges quickly and precisely enough to be used for simulating large PV arrays. The simulation model can accurately forecast steady-state performance given the inputs of solar irradiation level and PV module temperature.

5.2 Future Scope

Traditional PV array overcurrent protection relies on a circuit protection device (such as a fuse or circuit breaker) to automatically interrupt the fault current. However, it is challenging to adequately implement conventional protective devices due to the current-limiting nature of PV arrays. According to our research, line-line faults in PV arrays may result in new protection difficulties. For instance, even if a fault occurs under high irradiance, a line-line fault with a tiny voltage differential might not result in a high enough current to blow a fuse. Furthermore, fuses may not properly clear a line-line fault in low irradiance. Additionally, this "low irradiance" problem could develop during the transition from "night to day" and go undetected even at dawn and sunset. As a result, the flaws could be concealed in PV arrays and pose a risk to the efficiency and dependability of PV systems. However, these faults cannot be resolved by fuses because of their low fault current. An additional extension of the research would be to enhance fault finding and identification for massive PV arrays. Large, centrally located PV arrays have the drawback that it might be challenging to precisely locate the defect and determine the fault's type. It can occasionally be challenging for maintenance engineers or conventional PV monitoring systems to correctly pinpoint the fault in a large PV installation. One explanation for this is because when PV modules are electrically coupled, their performance is affected by one another.

References

[1] J. Wiles, Should They Be Grounded? - A series of articles on photovoltaic (PV) power systems and the National Electrical Code *IAEI NEWS*, 2004.

[2] J. A. Gow and C. D. Manning, "Development of a photovoltaic array model for use in power-electronics simulation studies," *Electric Power Applications, IEE Proceedings*, vol. 146, pp. 193-200, 1999.

[3] B. N. Nunneh, and A. A. Nur, "Levelized cost of Electricity (LCOE) for Solar Building Integrated Photovoltaic (BIPV) systems," *Zenodo*, 2021. https://doi.org/10.5281/zenodo.7394735

[4] A. B. Taha and S. F. Babiker, "Design and Simulation of Voltage Source Grid Connected Inverter (VSI)," *International Conference on Computer, Control, Electrical and Electronics Engineering (ICCCEEE)*, 2018.

[5] D. W. Hart, DC-DC Converters. In Power Electronics (pp. 211–216). , 1221 Avenue of the Americas, New York, NY 10020. The McGraw-Hill Companies, Inc. (2011).

[6] S. Salman**,** X. AI**,** and Z. WU, Design of a P-&-O algorithm based MPPT charge controller for a stand-alone 200W PV system. Renewable Energy Technologies for Sustainable Improvements 3(25), (2018) https://doi.org/10.1186/s41601-018-0099-8

[7] E. Roman, R. Alonso, P. Ibanez, S. Elorduizapatarietxe, and D. Goitia, "Intelligent PV module for grid-connected PV systems", Industrial Electronics, IEEE Transactions on Energy Conversion, vol. 53, issue 4, pp. 1066–1073, 2006.

[8] T. Takashima, J. Yamaguchi, K. Otani , T. Oozeki, K. Kato and M. Ishida, “Experimental studies of fault location in PV module strings,” Sol Energy Mater Sol Cells, vol. 93, pp. 1079-82, 2009.

[9] L. Schroon, F.P. Califano and M. Pastena, “Fault detection in a photovoltaic plant by time domain reflectometry,” ProgPhotovolt Res Appl., vol. 2, pp. 35-44, 1994.

[10] S. Vergura, G. Acciani, V. Amoruso and G. Patrono, “Inferential statistics for monitoring and fault forecasting of PV plants,” in proceedings of the IEEE international symposium, industrial electronics, Cambridge, UK. pp. 2414-19, 2008.

[11] A. Drews, A.C. de Keizer, H.G. Beyer, E. Lorenz, J. Betcke, and W.G.J.H.M van Sark, “Monitoring and remote failure detection of grid-connected PV systems based on satellite observations,” Solar Energy, vol. 81, pp. 548-64, 2007.

[12] M. Drif, A. Mellit, J. Aguilera, and Perez PJ, “A comprehensive method for estimating energy losses due to shading of GC-BIPV systems using monitoring data,” Solar Energy., vol. 86, pp. 2397-404, 2012.

[13] S. Syafaruddin, E. Karatepe, and T. Hiyama, “Controlling of artificial neural network for fault diagnosis of photovoltaic array,” in proceedings of the 16th international conference on intelligent system application to power systems (ISAP), Greece, pp. 1-6, 2011.

[14] P. Ducange, M. Fazzolari, B. Lazzerini, and F. Marcelloni, “An intelligent system for detecting faults in photovoltaic fields,” in proceedings of the IEEE 11th international conference on intelligent systems design and applications, Cordoba, Spain, pp. 1341-46, 2011.

[15] Y. Yagi, H. Kishi, R. Hagihara, T. Tanaka, S. Kozuma, and T. Ishida, “Diagnostic technology

and an expert system for photovoltaic systems using the learning method," Sol Energy Mater Sol Cells, vol. 75, pp. 655-63, 2003.

[16] S.K. Firth, K.J. Lomas, and S.J. Rees, "A simple model of PV system performance and its use in fault detection," Solar Energy, vol. 84, pp. 624-35, 2010.

[17] N. Gokmen, E. Karatepe, B. Celik, and S. Silvestre, "Simple diagnostic approach for determining faulted PV modules in string-based PV arrays," Solar Energy, vol. 86, pp. 3364-77, 2012.

[18] Y. Zhao, B. Lehman, J.F. DePalma, J. Mosesian, and R. Lyons, "Challenges to overcurrent protection devices under line-line faults in solar photovoltaic arrays," in proceedings of the IEEE energy conversion congress and exposition (ECCE), Phoenix, pp.20-27, 2011.

[19] K. H. Chao, S.H. Ho, and M.H. Wang, "Modelling and fault diagnosis of a photovoltaic system," Electrical Power System Research, vol. 78, pp. 97-105, 2008.

[20] X. Lin, "Online fault detection and tolerance for photovoltaic energy harvesting systems," in Proc. ICCAD, 2012.

[21] Y. Wang, "Enhancing efficiency and robustness of a photovoltaic power system under partial shading," in Proc. ISQED, 2012.

[22] N. Femia, "Optimization of perturb and observe maximum power point tracking method," IEEE Trans. Power Electronics, 2005.

[23] Y. Wang, "Charge migration efficiency optimization in hybrid electrical energy storage (HEES) systems," in Proc. ISLPED, 2011.

[24] S. K. Firth, “A simple model of PV system performance and its use in fault detection,” Solar Energy, 2010.

[25] M. G. Villalva, J. R. Gazoli, and E. R. Filho, "Comprehensive Approach to Modeling and Simulation of Photovoltaic Arrays," *Power Electronics, IEEE Transactions on,* vol. 24, pp. 1198-1208, 2009.

[26] R. C. Campbell, "A Circuit-based Photovoltaic Array Model for Power System Studies," in *Power Symposium, NAPS '07. 39th North American*, pp. 97-101, 2007.

[27] L. Schirone, “Fault finding in a 1 MW photovoltaic plant by reflectometry,” in Proc. WCPEC, 1994.

[28] X. Lin, “Near-optimal, dynamic module reconfiguration in a photovoltaic system to combat partial shading effects,” in Proc. DAC, 2012.